

**UNIVERSIDADE DE SÃO PAULO**

**PUBLICAÇÕES**

**INSTITUTO DE FÍSICA  
CAIXA POSTAL 66318  
05389-970 SÃO PAULO - SP  
BRASIL**

**IFUSP/P-1214**

**INFLUENCE OF RESONANT MAGNETIC  
PERTURBATIONS ON PLASMA EDGE  
TURBULENCE**

**R.M. Castro, M.V.A.P. Heller, I.L. Caldas, Z.A. Brasílio,  
R.P. da Silva, I.C. Nascimento**  
Inst. of Physics, Univ. of São Paulo,  
CP 66318, 05389-970, São Paulo, BRASIL

Abril/1996

# Influence of resonant magnetic perturbations on plasma edge turbulence.

R. M. Castro, M. V. A. P. Heller, I. L. Caldas, Z. A. Brasilio, R. P. da Silva,  
I. C. Nascimento.

Inst. of Physics, Univ. of São Paulo, C. P. 66318, 05389-970 São Paulo, SP, Brazil.

**ABSTRACT:** In this work we report alterations, on plasma-edge equilibrium profiles, edge turbulence, and anomalous transport, induced by resonant perturbing magnetic fields in the TBR tokamak [J. Fusion Energy 12, 295 (1993)]. Thus, these perturbations reduce the equilibrium parameters and the spectral power of the fluctuations, and enhance their phase velocity. They reduce also the particle flux at the plasma edge. All these electrostatic edge-parameters are computed taking into account temperature fluctuation corrections. Although the perturbation only slightly affects the linear correlation between magnetic and electrostatic fluctuations, their bispectral analysis shows a reduction of the quadratic mode coupling. Furthermore, the energy transferred between different spectral components, with and without the magnetic perturbation, have not the same direction for all fluctuations. Finally, the normal probability distribution functions of the fluctuations show significant non-Gaussian features. Nevertheless, the fluctuating potential distribution becomes near Gaussian with the magnetic perturbation.

Pacs Numbers: 5235R, 5270

## I. Introduction.

The interest in the control of the plasma-edge is based on the evidence that improvements of the plasma confinement depend on the edge behavior<sup>1,2</sup>. Remarkably, in the last years, experiments show that anomalous edge particle transport is induced by the electrostatic turbulence. Nowadays, the intensive investigation of edge turbulence and transport is motivated by the unexpected results obtained on large tokamaks<sup>2</sup>.

As originally proposed in the seventies<sup>3</sup>, the utilization of external magnetic perturbation is nowadays used in some tokamak devices to create a chaotic magnetic configuration, at the plasma edge, adequate to control particle and heat diffusion and, consequently, to improve the plasma confinement. Accordingly, the magnetic field lines at the plasma edge are made chaotic by applying resonant helical magnetic fields created by external resonant helical windings (RHW)<sup>4</sup> or ergodic divertors<sup>5-7</sup>. The expected effect of these perturbations is to produce uniform particle and heat loads to the wall along chaotic magnetic field lines. The resultant edge cooling reduces impurities, provides screening to impurity influx, and consequently improves confinement characteristics. However, the local effect of these resonant magnetic perturbations on the turbulence and its effect on the transport in the edge is still an open question<sup>8,9</sup>.

This paper reports the tentative of controlling the plasma edge turbulence with external electrical currents on the resonant helical windings wound on the TBR tokamak vessel<sup>10</sup>. So, it describes some observed alterations produced by these perturbations

on edge parameters, transport, and structures of magnetic field and electrostatic field fluctuations.

Other experiments in the TBR tokamak employing these resonant field perturbations, created by the RHW, have already been done to control MHD oscillations<sup>11</sup>, and to control turbulence with a field strength lower than that used in this work<sup>4</sup>.

In this experiment external coils create both magnetic islands and chaotic field regions through island overlapping<sup>12</sup>. Thus, we study the influence of the resonances created by the  $m = 4/n = 1$  RHW on the plasma edge turbulence (as usual,  $m$  and  $n$  determine the poloidal and toroidal wave numbers, respectively).

For a complete estimation of the anomalous particle transport in this turbulent plasma, it is necessary to measure density, potential, and temperature fluctuations, and the phases and correlations between these fluctuating quantities<sup>13,14</sup>. Thus, for the present investigation, a complex system of probes, which measures simultaneously electrostatic and magnetic fluctuations and some plasma mean parameters, was projected and installed at TBR. To improve the accuracy of these measurements, temperature fluctuations were also determined and taken into account to correct density and plasma potential fluctuations<sup>15</sup>.

To determine the influence of the magnetic perturbations on the linear and quadratic coupling between the measured fluctuations, the obtained data are treated with spectral and bispectral estimation methods<sup>16-21</sup>. For fluctuations monitored at two points in space we also estimate linear and quadratic transfer functions<sup>17,18</sup> to measure coupling coefficients, energy transfer, and, consequently, energy cascading throughout

the main oscillation frequency domains.

The analysis show that the magnetic perturbations reduce the equilibrium parameters and the spectral power of the fluctuations, and enhances their phase velocity. These perturbations produce also a reduction on the particle flux at the plasma edge. Complementary, the bispectral analysis shows that the RHW suppresses the quadratic coupling, whereas the power functions show no common specific direction for the fluctuation driven energy cascading, i.e., the energy transferred between different spectral components.

The conditions for the existence of intermittency in the measured signals are investigated with and without the perturbations induced by the RHW. In spite of that, no clear evidences of intermittent fluctuations are found, since the departure from a Gaussian distribution, a broadband power spectrum with no localized peaks, and the small time correlations are not simultaneously detected for the whole spectrum.

The relation between the temperature, potential, density, and magnetic fluctuations investigated in this work may contribute to identify the basic mechanisms determining edge turbulence<sup>22,23</sup>.

The outline of this paper is as follows: Section 2 gives a brief description of the apparatus and basic analysis techniques. In Section 3, we describe the behavior of temperature, density, plasma potential equilibrium, and fluctuation profiles, with and without RHW utilization. In section 4, we analyze the spectral and bispectral characteristics of the electrostatic turbulence and the behavior of the anomalous crossfield flux in the situation of section 3. In section 5, the characteristics of magnetic fluctu-

ations are studied with and without RHW and results of cross spectra and bispectral calculations between electrostatic and magnetic fluctuations are analyzed. Section 6 summarizes the conclusions of this work.

## II. Apparatus and Analyzing Techniques.

The experiment was carried out on the Ohmically heated TBR tokamak, with major radius  $R_o = 0.30$  m, minor radius  $a = 0.08$  m, toroidal magnetic field  $B = 0.4$  T, plasma current  $I_p \simeq 10$  kA, chord average density  $n_0 \simeq 7 \times 10^{18} \text{ m}^{-3}$ , and pulse length of  $10 \text{ ms}^{10}$ . The plasma in the TBR has a circular cross section and a full poloidal limiter. The used gas was hydrogen.

The data were collected from a multipin Langmuir probe, Fig.1, inserted into the plasma through a diagnostic port at the top of the tokamak,  $45^\circ$  toroidally displaced from the poloidal limiter<sup>15</sup>. This probe system was composed by four tips, a four-pin probe array and a single probe tip. Two of the four pin configuration measures the floating potential fluctuations,  $\bar{\varphi}_f$ , and the other two measure the ion saturation current fluctuations,  $\bar{I}_{si}$ . These two pairs of pins were used for determining the spectrum,  $S(k, f)$ , the power weighted average values of poloidal wave vector,  $k_\theta$ , the phase velocity,  $v_{ph}$ , and the width of the  $k_\theta$ <sup>24</sup>. Another single tip, at  $3\text{mm}$  from the four tip configuration, was used to directly measure the mean value of the floating potential,  $\varphi_f$ .

The electron mean temperature,  $T_e$ , its fluctuation,  $\bar{T}_e$ , the ion saturation current,  $I_{si}$ , and its fluctuation,  $\bar{I}_{si}$ , were obtained using a modified triple probe technique<sup>15,25-27</sup> with four pins for phase delay error corrections. Mounted in the same

system, two sets of two magnetic coils, Fig.1, measured poloidal,  $\dot{B}_\theta$ , and radial,  $\dot{B}_r$ , components of magnetic field fluctuations. From these coils we determine the radial profiles of the magnetic field components, the poloidal wave vector, the phase velocity, and the ratio between magnetic and electrostatic fluctuations.

The probe measurements were done during the flat top phase of the plasma current (Fig.2), in time intervals of approximately  $4 \text{ ms}$  and averaged throughout seven consecutive shots. The time series measurements were recorded using 8 bit digitizers, with a maximum sampling rate of  $1 \text{ Mhz}$ . The length of the used data consisted of 105 samples of 256 points. These series were submitted to a statistical criterion to eliminate spurious points that otherwise would contribute to over estimate the fluctuations.

The plasma density was obtained by  $n \propto I_{si}/T_e^{1/2}$ . The quantities measured with the triple probe were decomposed, using a numerical filter, into mean ( $f < 5 \text{ kHz}$ ) and fluctuating ( $5 \text{ kHz} < f < 500 \text{ kHz}$ ) parts.

Density and potential fluctuations corrected by temperature fluctuations were obtained by<sup>27</sup>:

$$\bar{n} = n[\bar{I}_{si}/I_{si} - \bar{T}_e/2T_e + (\bar{T}_e/2T_e)^2] \quad (1)$$

and

$$\bar{\varphi}_p = \bar{\varphi}_f + \sigma K \bar{T}_e/e, \quad (2)$$

where  $\sigma$  is considered equal to  $2.8^{15}$ . The plasma potential ( $\varphi_p$ ) is related to floating

potential ( $\varphi_f$ ) through an equation similar to Eq. 2.

The external magnetic field perturbation were created by electric currents circulating in a set of helical windings located externally around the torus<sup>28</sup>. These coils produced a perturbation field with dominant helicity  $m = 4/n = 1$  and average radial amplitude  $\langle |\dot{B}_r(a)/\dot{B}_\phi| \rangle \simeq 0.4\%$  at the limiter radius ( $B_\phi$  is the toroidal equilibrium field, and  $B_r$  the radial perturbing field). This perturbation was resonant once the edge safety factor  $q \leq 4$ . The currents circulating in these coils were adjusted to  $I_h = 285 A$  and they were switched on after the plasma current had reached steady values, Fig.2.

These coils created both magnetic islands and ergodic field regions through island overlapping. Fig.3 shows the Poincaré maps computed for those discharges with a dominant  $m/n = 2/1$  MHD mode with, Fig.3a, and without, Fig.3b, the resonant perturbations created by the  $m/n = 4/1$  helical windings. While in the unperturbed map, Fig.3b, the  $m/n = 2/1, 3/1$  and other smaller islands can be recognized, the applied field destroyed the magnetic surfaces in an ergodic layer of about  $1.5 \times 10^{-2} m$  radial width at the plasma edge, Fig.3a. This ergodic region did not include the  $q = 2$  islands and it was created around the unperturbed magnetic surface with the safety factor  $q = 4$ . In this case the stochasticity parameter, computed for the  $m/n = 3/1$  and  $m/n = 4/1$  island superposition, was  $s \simeq 1^{12}$ . Thus, in this experiment the RHW created a field line configuration similar to those obtained in the tokamak TEXT<sup>5</sup> and TORE SUPRA<sup>7</sup> with ergodic divertors.

### III. Equilibrium and Fluctuation Profiles.

In the analyzed experiments, the resonant magnetic perturbation created by the helical windings change remarkably the equilibrium parameters and fluctuating quantities at the plasma edge.

A sharp temperature gradient exists without the RHW utilization, Fig.4a. With the RHW the radial temperature profile became flat from  $r/a = 0.81$  till  $r/a = 0.96$ . The existence of this modified flat profile suggests the formation of a layer where the thermal diffusivity is controlled by the chaotic field lines, as it was observed in the Tore-Supra tokamak<sup>7,8</sup>. The density profile also decreases, Fig.4b, and this behavior is attributed to the different connection to the walls created by the RHW perturbation resulting in a larger area seen by the plasma. Similar alterations were also induced by an ergodic divertor in the Tore Supra tokamak<sup>7,8</sup>.

During RHW operation the floating potential and plasma potential profiles, Figs. 5a-b, were also modified. The utilization of the magnetic perturbation turned the floating potential less negative, specially near the region  $r/a = 0.85$ , where the effect was clearly seen. Consequently, since the plasma potential profile was lowered and smoothed by the perturbation, the radial electric field,  $E_r$ , decreased.

The plasma potential is positive in the measured region; this result was also observed in the TEXT tokamak<sup>29</sup> for reduced equilibrium parameter discharges. Furthermore, the variation of  $E_r$  shows the absence of a shear layer, confirmed also by the measured profile of phase velocity. As already mentioned, there is no experimental evidence of the existence of any shear layer in the TBR plasma edge<sup>15,28</sup>. The

results of this work, compared with previous measurements<sup>28</sup>, show that the changes in the mean parameters profiles induced by external perturbations increases with the perturbing field strength.

Fig.6 shows the radial profiles of electron temperature fluctuation rms amplitudes normalized to local mean value, with and without utilization of RHW. Although the equilibrium and fluctuating temperature were altered by the utilization of the RHW, no noticeable effect was detected on the ratio between these two measurements. In the same figure are also the normalized plasma potential fluctuation profiles; here a significant alteration is noted only at the limiter position. Furthermore, the general level of density turbulence,  $n_e^{rms}/n_e$ , remained approximately constant when the resonant field was activated.

In a plasma current scan from 6 kA to 10 kA, for a constant position  $r/a = 0.89$  of the probe system, we observed a steep increase of the mean value of density,  $n$ , and plasma potential,  $\varphi_p$ , without the RHW. On the other hand, no noticeable alteration was detected in the mean temperature,  $T_e$ . Although this behavior of the  $n$  and  $\varphi_p$  profiles during the plasma current scan was the same with the RHW, even so, the previously described effect of lowering the mean parameters was ratified with the RHW utilization.

For the mentioned scan of plasma current, the relative level of the density and temperature fluctuations remained constant even with the utilization of the RHW. On the other hand, the relative level of the plasma potential fluctuations decreased with the plasma current increment. Finally, the utilization of external magnetic

perturbations during the current scan did not affect the plasma potential fluctuation level.

The observed profiles showed that the external magnetic perturbation produced changes in the edge plasma structure, specially in the equilibrium parameters.

#### IV. Electrostatic Turbulence and Transport.

To study the effect of RHW on particle transport we investigated the changes in the plasma edge parameters that are commonly associated with that transport.

Thus, digital spectral analysis is used to compute the spectral power density distribution function  $S(k, f)$ <sup>24</sup>, for density and fluctuating potential time series. Fig.7, shows the  $S(k, f)$  spectra for density fluctuations at the radial position  $r/a = 0.89$ , computed for discharges without magnetic perturbation, Fig.7a, and for perturbed discharges, Fig.7b. Spectral density functions are strongly decreased by the RHW. These spectra show that both the wave vector component,  $k_\theta$ , and its spectral width,  $\sigma_{k_\theta}$ , are reduced by the RHW utilization. This reduction corresponds to a global decrease of the fluctuations and, since the low wave numbers are dominant in the spectrum, this suggests a turbulence stabilization. Although not so marked, the same kinds of alterations were also produced by the RHW on the plasma potential spectra.

Fig.8 shows the phase velocity profiles for plasma potential fluctuations with and without magnetic perturbations. Inside the plasma, the poloidal phase velocity is essentially in the same direction as the ion diamagnetic drift velocity. The effect of the RHW is to enhance the phase velocity because of the reduction of the average

wave vector. The absence of shear layer already reported<sup>15,28</sup> is confirmed in this new experiment.

To determine a possible relationship between the measured fluctuations, the cross spectra of these fluctuations were computed. The results show that the influence of the magnetic perturbations is overall to enhance the correlation between the temperature, the ion saturation current, and the floating potential fluctuations.

Evaluations of the convected and the conducted energy fluxes at the limiter show that they are very low compared with the total power input<sup>15</sup>, so the power flux should be dominated by other losses, such as radiation. Even though, the magnetic perturbation further reduces these two kinds of energy fluxes.

In this work, the driven particle flux,  $\Gamma$ , is calculated by<sup>30</sup>:

$$\Gamma = \int 2k_{\theta} P_{n\varphi} \sin(\theta_{n\varphi}) / B_{\phi} df \quad (3)$$

Fig.9 shows the particle flux profiles for discharges with and without the RHW perturbation. An appreciable alteration was produced in the plasma edge transport by the utilization of resonant perturbations, at this field strength. The results show not only a reduction of the particle flux in the whole spectrum but even, for some low frequency intervals, an inversion in its radial direction. In the literature, this inward transport at low frequencies has been associated with drift wave fluctuations driven by ionization effects<sup>31,32</sup>.

From the radial distribution of electron density at the plasma edge we can roughly estimate the radial diffusion coefficient across the main magnetic field under the effect

or not of the applied perturbations. The diffusion coefficient,  $D$ , is given by

$$D = -\Gamma / \nabla n \quad (4)$$

where  $\Gamma$  is the particle flux. Results obtained near the limiter give  $D \simeq 0.3 \text{ m}^2/\text{s}$ . Even so the perturbing magnetic field seems to enhance slightly the diffusion coefficient at the plasma edge, the computed difference is almost within the experimental errors of the measured quantities. Thus, at least from our results, even with the previously described variations of  $\Gamma$  and  $\nabla n$ , we cannot assure that the RHW perturbation increases the radial diffusion coefficient

To understand the experimental results related to particle transport in the presence of resonance fields, we compare the diffusion coefficient previously computed from the data with the following theoretically predicted under the conditions of the described experience<sup>6</sup>. Thus, in the collisionless plasma limit with a stochastic field, the following expression can be used to estimate the diffusion coefficient,  $D^C$ :<sup>6</sup>

$$D^C = \langle D_m \rangle v_{thi} \quad (5)$$

where  $D_m$  is the magnetic diffusion coefficient of the chaotic field lines given by:

$$D_m = \pi R \langle |B_r / B_{\phi}|^2 \rangle \quad (6)$$

The ion thermal velocity,  $v_{thi}$ , is estimated by considering the average values of the plasma edge temperatures, near the limiter,  $T_i \simeq T_e \simeq 15 \text{ eV}$ , as usually. Thus,

we obtain  $D^C \simeq 0.27 \text{ m}^2/\text{s}$ , as the average radial diffusion coefficient in this region.

This value is in good agreement with the experimental diffusion coefficient  $D$ .

Another expression that can be used in the collisional low stochasticity limit is<sup>6</sup>:

$$D^N = 0.3 \langle B_r/B_\phi \rangle \lambda_n c_s \quad (7)$$

where  $\lambda_n$  is the density scale length,  $c_s$  is the ion sound speed, and 0.3 is a factor used to account for similar experimental observations in magnetic limiter<sup>6</sup> and divertor experiments<sup>33</sup> as suggested in Ref. 34. Estimations of  $D^N$  for the same region give  $D^N \simeq 0.05 \text{ m}^2/\text{s}$ , a result in disagreement by one order of magnitude with the value obtained from the data.

One way to investigate the nonlinear coupling among different fluctuation components is to use the bispectral analysis technique as suggested in Refs. 16,19. In the present analysis the recorded data are not enough to neglect the variance of the bicoherence ( $b^2$ ). It has been shown that the variance of bicoherence<sup>35</sup> is estimated as  $\sigma_{b^2} \simeq 2b/M^{1/2}$  (where  $M = 210$  is the number of successive realizations with intervals of  $128 \mu\text{s}$ ). Considering the autobicoherence of floating potential, ion saturation current, and temperature fluctuations, no prominent peaks can be identified. However, a low level of nonlinear coherent interactions (much larger than the statistical uncertainty) is clearly observed in the bispectral analysis, showing that nonlinear coupling exists in the edge electrostatic fluctuations.

Fig.10 shows the bicoherence of  $I_{si}$  fluctuations at  $r/a = 0.92$ , with (a) and without (b) the RHW utilization. The maximum value is  $b^2 = 0.24 \pm 0.03$  for the

case (a) and  $b^2 = 0.40 \pm 0.05$  for the case (b). For the unperturbed oscillations, Fig.10 (b), the nonlinear interactions are concentrated mainly at  $f_2 \leq 50 \text{ kHz}$  and  $f_1 \leq 120 \text{ kHz}$ . However, the presence of the magnetic perturbations lower the bicoherence values and alter the frequency regions to  $f_2 \leq 20 \text{ kHz}$  and  $f_1 \leq 50 \text{ kHz}$ . A similar situation is observed for the other parameter fluctuations.

Fig.11 shows the integrated bicoherence for the same fluctuations of Fig.10 with and without the resonant fields. The computed values decreased with the magnetic perturbation. Furthermore, we observe the highest bicoherence values for components at 50 and 100 kHz. Considering any of these two frequency components satisfying the resonant condition  $f = f_1 + f_2$ , the bicoherence (for interactions with and without RHW) does not present any contribution from modes of the high frequency band.

The crossbicoherence between the considered fluctuating parameters shows no prominent peaks, but the values are larger than the statistical uncertainty. However, the utilization of the RHW lower the crossbicoherence values to approximately the statistical uncertainty.

To evaluate the nonlinear coupling coefficients and the amount of energy cascading between waves, we utilize the method proposed in Refs. 17,18. The relationship between fluctuations monitored at two points in space is described with linear and quadratic transfer functions. From these we can compute the growth rate, the dispersion relation, the wave-wave coupling coefficient, and the energy transfer between spectral components<sup>15</sup>.

Overall, the systematic calculation of the growth rate of the electrostatic fluctu-



tuations show negative values correspondents to a linear damping mechanism. An almost linear dispersion relation is observed for the low frequency components. The RHW does not introduce any significant difference in the frequency dependence of the growth rate and the dispersion relation.

The amplitude of the coupling coefficient that gives the strength of coupling, leading to the decay of the wave of frequency  $f$ , into waves of frequencies  $f_1$  and  $f_2$  or to the merging of two waves into one, is not significant with and without RHW.

For floating potential fluctuations the power transfer function shows that the difference interaction region was dominated by negative transfer rates. For ion saturation current fluctuations the power transfer function is much lower and presents no preferential direction. The fluctuating potential fluctuations perturbed by the RHW presents a positive power transfer in the difference interaction region.

Analyzing the values of higher order moments of the data, such as skewness and kurtosis, we observe no clear evidence of Gaussian probability distribution functions for the electrostatic fluctuations with and without the magnetic perturbation. Thus, Fig.12a,b shows non-Gaussian probability distribution functions obtained for the ion saturation current fluctuations. In these cases the signal has an almost zero value for skewness, but the kurtosis values differ significantly from three (the value corresponding to Gaussian distributions). The RHW do not alter these distributions. However, in the case shown in Fig.12b,c for fluctuating potential fluctuations, the magnetic perturbations alter significantly the distribution that became similar to a Gaussian one. Finally, the time correlations are small, nearly  $4\mu s$ , and do not show any change

with the RHW.

## V. Magnetic Fluctuations.

The magnetic fluctuations on surfaces inside the plasma are detected by pick-up coils located behind the limiter. The amplitude and phase of these fluctuations can be compared with the previously analyzed electrostatic parameters to determine any possible correlation between these two kinds of oscillations and, consequently, between the magnetic oscillations and the anomalous transport during the TBR discharges.

Although the magnitude of the fluctuation is higher for the poloidal field than for the radial field, these field components have similar spectra. In addition, as previously reported<sup>28</sup>, in the TBR the main frequencies observed in the electrostatic power spectra are smaller than the Mirnov frequencies. Furthermore, the frequency power spectra of these oscillations still have a marked partial superposition. These two last particular characteristics of the fluctuations in TBR encourage the investigation of any possible correlation between the electrostatic and the magnetic oscillations. These TBR features are observed in discharges with and without the RHW utilization. Fig.13 shows, in the case of RHW utilization, this peculiar partial superposition of density, plasma potential, and magnetic poloidal fluctuations measured at  $r/a = 0.81$  (for electrostatic fluctuations) and at  $r/a = 1.03$  (for poloidal magnetic fluctuations). This peculiarity can offer a unique condition to investigate linear and quadratic correlation between electrostatic and magnetic fluctuation spectra's components in tokamaks.

As expected<sup>11,36,37</sup>, the RHW reduces the magnetic field fluctuation amplitudes. This effect can be seen in Fig.14 that shows the  $B_{\theta}^{rms}$  values, for discharges with and without the RHW utilization, normalized to the equilibrium magnetic poloidal field value at the limiter.

The correlation analysis shows that the magnetic fluctuations detected by the poloidal or the radial oriented coils are very well correlated. In fact, the coherence is higher than 0.9 for the regions with higher spectral density. The phase angle, approximately equal to  $\pi/6$ , between the fluctuations obtained from two poloidal coils is almost the same of that obtained with two radial coils. The utilization of resonant magnetic fields do not change the phase angle between radial magnetic fluctuations, but for the perturbed poloidal fluctuations we detect a phase angle near zero, an indication of a possible standing wave pattern in the poloidal direction. The utilization of the external perturbations do not change the phase angle, approximately equal to  $\pi/2$ , between the poloidal and the radial fluctuations.

Since the specially constructed edge probe array permits simultaneous two point measurements of electrostatic and magnetic fluctuating quantities, we compared their propagation characteristics and investigate the relation between these oscillations.

The propagation characteristics of  $\tilde{B}_r$  and  $\tilde{B}_\theta$  are similar to those of electrostatic fluctuations, because the dispersion is linear in the region of high spectral power density and  $\sigma_k/k > 1$ . Propagation velocities for magnetic fluctuations are always in the electron drift direction. They are much higher than those of electrostatic fluctuations, as in other tokamaks<sup>38</sup>.

The RHW utilization raises the value of phase velocity of the magnetic fluctuations. Calculations near the limiter give  $v_{B\theta} \approx -9.0 \times 10^3 m/s$ , without RHW, and  $v_{B\theta} \approx -13.0 \times 10^3 m/s$  with RHW. These results come from the high power magnetic fluctuations with  $k$  values lower than those measured for the electrostatic fluctuations.

Next step is to investigate the linear correlation between electrostatic and magnetic fluctuations, and the influence of external perturbations on this correlation. For the region of high-power density, the average coherence between temperature fluctuations and poloidal or radial magnetic fluctuations is almost uniform,  $\gamma \approx 0.4$ , in the plasma edge. The coherence between magnetic fluctuations and electrostatic fluctuations is, for the same high-power density region,  $\gamma \approx 0.3$ .

The perturbation caused by the RHW produces, in the plasma edge, a small lowering of coherence between the considered parameters.

Using the model suggested in ref. 38, to link the computed average coherence  $\gamma$  with the fraction of magnetic fluctuation power attributed to the electrostatic turbulence, the expression for the magnetic fluctuation signal is given by:

$$\tilde{B}_\theta(f) = S_{EL}(f) + N(f), \quad (8)$$

where  $S_{EL}$  is the magnetic signal due to the local electrostatic fluctuation and  $N(f)$  is the magnetic noise element. From this reference, we can relate the previously computed coherence between the magnetic and the electrostatic fluctuations with the ratio  $S_{EL}/N$ :

$$\gamma(f) = (1 + (S_{EL}/N)^{-2})^{-1/2} \quad (9)$$

Then, a maximum of  $\gamma \approx 0.4$  still corresponds to only  $(S_{EL}/N)^2 \approx 0.2$ . Therefore, in our case a relatively low fraction of the magnetic fluctuation power could be associated to the local electrostatic fluctuation ( $\approx 20\%$ ).

Using the bispectral analysis, by inspection of the autobicoherence of poloidal magnetic fluctuations, we concluded that the nonlinear interactions are concentrated mainly in the frequency intervals  $10 \approx < f_1 \approx < 60 \text{ kHz}$  and  $10 \approx < f_2 \approx < 50 \text{ kHz}$ . Furthermore, without RHW utilization, they have a significant level larger than the statistical uncertainty.

The integrated bicoherence is significative for the frequencies in the MHD region around  $50 \text{ kHz}$ . Here, modes of the broadband high frequency do not satisfy the resonant condition  $f_1 \pm f_2 = 50 \text{ kHz}$ . Thus, for the magnetic oscillations, there is no evidence of coupling between the macroscopic modes and the turbulent oscillations. The effect of magnetic perturbations is to reduce the value of the integrated bicoherence, but the general aspects already mentioned are preserved.

The crossbicoherence between the poloidal magnetic fluctuations measured by two different coils is more significative without RHW. The highest value of the nonlinear coupling appears between modes with  $f \approx 250 \text{ kHz}$  and  $f_1 - f_2 \approx 100 \text{ kHz}$ .

The crossbicoherence between poloidal magnetic fluctuations and electrostatic fluctuations is significative for temperature and ion saturation current fluctuations. The highest value appears in the same frequency region of the cross coherence peak

observed for the two poloidal magnetic coils. For poloidal magnetic and fluctuating potential fluctuations crossbicoherence is negligible. Here, the RHW has also the effect almost to suppress crossbicoherence.

For the high power density modes, the growth rate calculated for two magnetic coils is negative, showing the existence of a damping mechanism. No change in this damping is produced by the external magnetic perturbation.

The amplitude of quadratic coupling coefficient is high without magnetic perturbations. The most efficient coupling is observed for the sum interacting modes  $f_1 + f_2 \approx 80 \text{ kHz}$  and involves spectral components with frequencies  $|f_2| \leq 30 \text{ kHz}$  and  $f_1 \approx 50 \text{ kHz}$ . The RHW reduces the quadratic coupling coefficient and the frequency coupling range.

The power transfer function calculated for  $B_\theta$  presents only positive power transfer rates in the difference interaction region. The RHW reduces the power transfer function to negligible values.

For the magnetic fluctuations the calculation of skewness and kurtosis give mean zero values for skewness but high values for kurtosis. The RHW enhances the high values for kurtosis.

The correlation time is of the same order than for the electrostatic fluctuations, which is a small value compared with the time scale of the experiment and with the fluctuation time scale.

## VI. Conclusions.

In this work we present evidences of partial correlations between the electrostatic

and magnetic fluctuations at the plasma edge turbulence of the tokamak TBR. Relevant alterations on the spectra of these oscillations and on the electrostatic driven transport were observed after the edge magnetic structure, perturbed by the external resonant helical fields, became predominantly chaotic.

It is noticeable that in TBR not only the magnetic oscillations were strongly reduced, as in other experiments<sup>11,36,37</sup>, but also the electrostatic were slightly modified by the resonant helical windings used to perturb the magnetic field. This last effect could be associated to the uncommon (in tokamaks)<sup>1</sup> partly similar frequency spectra for these two kinds of oscillations. In fact, although the electrostatic power spectra present frequencies lower than the Mirnov frequencies, they still show a partial superposition with the magnetic power spectra. Therefore, in TBR, altering routinely the magnetic fluctuations to control the turbulence spectra at the plasma edge may be possible.

Recently, evidences of this kind of control were also reported for the Reversed Field Pinches (RFP)<sup>39,40</sup>. However, besides our present observations, the magnetic and the electrostatic oscillations do not have the same dominant driven processes, as it was suggested for the RFP, since the spectral analysis showed that only a relatively low fraction of the magnetic fluctuation power, not more than 20%, could be associated to the electrostatic fluctuation power.

Other examples of this influence can be mentioned, such as the modulation of the electrostatic turbulence by a dominant MHD mode<sup>41</sup>, and the correlations between the magnetic turbulence and the electrostatic transport<sup>42,43</sup>.

In TBR, these observations were obtained by using a special designed probe system that could measure simultaneously the amplitude and the phase of these fluctuations. In fact, the data were collected with a system of Langmuir probes: four tips, a four pin probe array, a single probe tip, and two sets of two magnetic coils. Thus, the mean and fluctuating values of the saturation current, floating potential, temperature, radial and poloidal magnetic field components were measured during discharges with and without the application of a resonant magnetic field.

A strong decrease of the measured equilibrium parameter profiles was observed with the utilization of the RHW. With the magnetic perturbation, the temperature profile became flat, suggesting the formation of a layer where the thermal diffusivity would be controlled by the chaotic field lines<sup>8</sup>. The observed changes of the electron temperature profile with the RHW utilization might produce modifications of the plasma current density gradient allowing a possible suppression or stabilization of the internal resistive modes<sup>36,44-46</sup>. Consequently, this effect might contribute to the observed decrease of the turbulence fluctuation at the plasma edge. The density profile also decreased in discharges perturbed by the RHW since the chaotic field line diffusion to the walls increased<sup>47</sup>.

Besides all the mentioned alterations on the mean and the fluctuating values, the ratios between these quantities, or specifically the level of density ( $n_e^{rms}/n_e$ ), temperature ( $T_e^{rms}/T_e$ ), and potential ( $e\varphi_p^{rms}/kT_e$ ) remain approximately constant when the resonant field is activated.

The plasma potential radial profile is lowered and smoothed by the perturbation,

consequently the radial electric field  $E_r$  decreased monotonically. This radial variation of  $E_r$  reinforces the previous measurements<sup>28</sup> that show the absence of a shear layer in the TBR discharges.

In a plasma current scan, for a constant position of the probe system and without the helical perturbation, we observed a steep increase of the mean value of density and plasma potential, and no significative alteration of the mean temperature. The utilization of the RHW maintains the same dependence of the measured parameters on the plasma current, but with a lowering of the mean values. Furthermore, this current scan do not produce any appreciable changes in the relative density and temperature fluctuation levels. Only the potential fluctuation amplitude decreases with increasing plasma current, and this behavior do not depend on the external magnetic perturbation.

Spectral power distribution functions  $S(k, f)$  of the fluctuating parameters decreased with the RHW perturbation. Since both the wave vector component and its spectral width are reduced, this reduction corresponds to a global decrease of the turbulence level.

The phase velocities of electrostatic fluctuations inside the plasma are essentially in the direction of the ion diamagnetic drift velocity. The effect of the RHW perturbation is to enhance the phase velocity because of the reduction of the average wave vector. On the other hand, propagation velocities for magnetic fluctuations are always in the electron drift direction and are much higher than electrostatic fluctuations. The RHW utilization also raises the magnetic fluctuation phase velocity.

The influence of the external perturbations is to enhance the linear correlation between the electrostatic fluctuations. However, the introduction of the RHW produces a small lowering of linear coherence between the magnetic and the electrostatic fluctuations.

The utilization of the RHW produces also a significant alteration on the particle flux profiles at the plasma edge. The particle flux shows not only a reduction but even, for some low frequency components, an inversion in its radial direction. However, this inward transport produces only a small overall effect on the frequency integrated transport. Theoretical studies show that the drift wave fluctuations driven by ionization effect could generate the observed inward transport<sup>31</sup>.

The particle diffusion coefficients calculated from the particle flux and density edge gradient for discharges with and without RHW show no remarkable differences. These diffusion coefficients are compared with some theoretical models; however, only the coefficient computed considering the randomization of the field lines gives values compatible with our results.

To investigate nonlinear coupling we used bispectral analysis. Thus, the auto-bicoherences of electrostatic fluctuations showed no prominent peaks; however, a low level of nonlinear coupling was clearly observed. The same is valid for the magnetic fluctuations. The effect of the magnetic perturbations is to reduce these bicoherences for all measured oscillations.

The crossbicoherence between two point data of electrostatic fluctuations and the crossbicoherence between two magnetic coils showed the same situation observed for

the autobicoherence. Another effect of the RHW is to lower the nonlinear coupling.

However, the crossbicoherence between the electrostatic and the poloidal magnetic fluctuations is significant only for the ion saturation current or the temperature fluctuations. The highest value appears in the same frequency region of the cross coherence peak observed for the two poloidal magnetic coils. Here, the RHW has also the effect almost to suppress this crossbicoherence.

The systematic calculation of the growth rate of the electrostatic and the magnetic fluctuations show negative values corresponding to a linear damping mechanism. Furthermore, the RHW does not introduce any significant alteration in these spectra.

For the electrostatic fluctuations, the amplitude of the quadratic coupling coefficient is not significant with and without the RHW. On the other hand, for the non perturbed magnetic fluctuations this coefficient is high. In this last case, the RHW reduces not only the coupling coefficient but also the frequency coupling range.

The power transfer function shows that for floating potential fluctuations the transfer of energy occurs in the negative direction, i.e., from high to low frequency modes. The RHW reverses this direction. For ion saturation current fluctuations the power transfer functions are much lower and present no preferential direction. For the magnetic fluctuations the transfer of energy occurs in the positive direction. Generally, this quadratic coupling is reduced by the RHW.

Analyzing the values of higher order moments of the data, such as skewness and kurtosis, for both the electrostatic and the magnetic fluctuations, we observed, with and without the magnetic perturbation, no clear evidence of Gaussian probability

distribution functions.

This reported analysis is not yet conclusive to prove the existence of intermittency in the fluctuating parameters measured at the TBR plasma edge, for discharges with and without RHW. The small correlation time and high values for kurtosis seem to agree with the existence of intermittency in the data, but as the measured fluctuating parameters exhibit some significant peaks in their autospectra, we think that we do not have a sufficient number of evidences. To prove the intermittency we are working in a more detailed analysis using correlation and conditional averaging techniques<sup>48</sup>.

*Acknowledgments:* The authors would like to thank the fruitful discussions with Dr. F. Karger and Dr. D. Biskamp (Max-Planck-Institut für PlasmaPhysik, Germany), Dr. R.D. Bengtson and Dr. S. McCool (Fusion Research Center, The University of Texas at Austin, USA). The authors are also thankful to Ms. Gisele Oda for computing the Poincaré maps shown in this work, and to Dr. A.N. Fagundes and Mr W.P. Sá (University of São Paulo, Brazil) for their computational assistance. This work was partially supported by the Brazilian research agencies FAPESP and CNPq.

## REFERENCES

- <sup>1</sup> A. J. Wootton, B.A. Carreras, H. Matsumoto, K. McGuire, W.A. Peebles, Ch. Ritz, P.W. Terry, S.J. Zweben, Phys. Fluids B2, 2879 (1990).
- <sup>2</sup> F. Wagner, U. Stroh, Plasma Phys. Control. Fusion, 35, 1321 (1993).
- <sup>3</sup> F. Karger, K. Lackner, Phys. Lett. A61, 385 (1978).
- <sup>4</sup> R. M. Castro, M.V.A.P. Heller, I.L. Caldas, R.P. da Silva, Z.A. Brasílio, Il Nuovo

- <sup>5</sup> S. C. McCool et al. *Nuclear Fusion* **29**, 547 (1989).
- <sup>6</sup> S. C. McCool, A. J. Wootton, M. Kotschenreuther, A. Y. Aydemir, R. V. Bravenec, J. S. DeGrassie, T. E. Evans, R. L. Hickok, B. Richards, W. L. Rowan, P. M. Schoch., *Nucl. Fusion* **30**, 167 (1990).
- <sup>7</sup> A. Grosman, P. Gendrih, C. DeMichelis, P. Mourier-Garbet, J. C. Vallet, H. Capes, M. Chatelier, T. E. Evans, A. Géraud, M. Goniche, C. Grisolia, D. Guilhem, G. Harris, W. Hess, F. Nguyen, L. Poutchy, and A. Samain, *J. Nucl. Mater.* **196**, 59 (1992).
- <sup>8</sup> J. Payan et al., *Nucl. Fusion*, **35**, 1357 (1995).
- <sup>9</sup> T. C. Hender, R. Fitzpatrick, A. W. Morris, P. G. Carolan, R. D. Durst, T. Edlington, J. Ferreira, S. J. Fielding, P. S. Haynes, J. Hugill, I. J. Jenkins, R. J. La Haye, B. J. Parham, D. C. Robinson, T. N. Todd, M. Valovic, G. Vayakis, *Nucl. Fusion* **32**, 2091 (1992).
- <sup>10</sup> I. C. Nascimento, I. L. Caldas, and R. M. O. Galvão, *J. Fusion Energy* **12**, 295 (1993).
- <sup>11</sup> A. Vannucci, O. W. Bender, I. L. Caldas, I. H. Tan, I. C. Nascimento, E. K. Sanada, *Il Nuovo Cimento* **10D** 1193 (1989)
- <sup>12</sup> A. S. Fernandes, M. V. A. P. Heller, I. L. Caldas., *Plasma. Phys. and Controlled Fusion* **30**, 1203 (1988).
- <sup>13</sup> W. Horton, *Phys. Rep.* **192**, 1 (1990).
- <sup>14</sup> J. D. Callen, *Phys. Fluids* **B4**, 2142 (1992).
- <sup>15</sup> R. M. Castro, M. V. A. P. Heller, I. L. Caldas, R. P. da Silva, Z. A. Brasilio, and

- I. C. Nascimento, *Phys. Plasmas* **3**, 971 (1996).
- <sup>16</sup> Y. J. Kim and E. J. Powers, *IEEE Trans. Plasma Science* **PS-7**, 120 (1979).
- <sup>17</sup> Ch. P. Ritz, E. J. Powers, *Physica* **1D20**, 320 (1986).
- <sup>18</sup> Ch. P. Ritz, E. J. Powers, and R. D. Bengtson, *Phys. Fluids* **B1**, 153 (1989).
- <sup>19</sup> K. Rypdal and F.ynes, *Phys. Lett.* **A184**, 114 (1993).
- <sup>20</sup> T. Estrada, E. Sanches, C. Hidalgo, B. Brañas, and C.P. Ritz, Proc. 20th EPS Conference on Controlled Fusion and Plasma physics (Lisbon, 1993), *Europhysics Conference Abstracts* **17C**, Part 1, p. 373.
- <sup>21</sup> H. Y. Tsui, K. Rypdal, Ch. P. Ritz, and A. J. Wootton, *Phys. Rev. Lett.* **70**, 2565 (1993).
- <sup>22</sup> D. Biskamp, *Nonlinear Magnetohydrodynamics*, Cambridge University Press, Cambridge (1993).
- <sup>23</sup> S. J. Camargo, H. Tasso, *Phys. Fluids* **B4**, 1199 (1992).
- <sup>24</sup> S. J. Levinson, J. M. Beall, E. J. Powers, and R. D. Bengtson, *Nucl. Fusion* **24**, 527 (1984).
- <sup>25</sup> H. Ji, H. Toyama, K. Yamagishi, S. Shinohara, A. Fujisawa, and K. Miyamoto, *Rev. Sci. Instrum.* **62**, 2326 (1991).
- <sup>26</sup> H. Ji, H. Toyama, K. Miyamoto, S. Shinohara, and A. Fujisawa, *Phys. Rev. Lett.* **67**, 62 (1991).
- <sup>27</sup> H. Y. Tsui, R. D. Bengtson, G. X. Li, H. Lin, M Meier, Ch. P. Ritz, and A. J. Wootton, *Rev. Sci. Instrum.* **63**, 4608 (1992).
- <sup>28</sup> M. V. A. P. Heller, R. M. Castro, Z. A. Brasilio, I. L. Caldas, and R. P. da Silva,

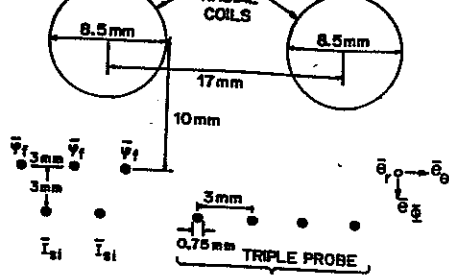


Fig. 1 - Scheme of probe assembly.

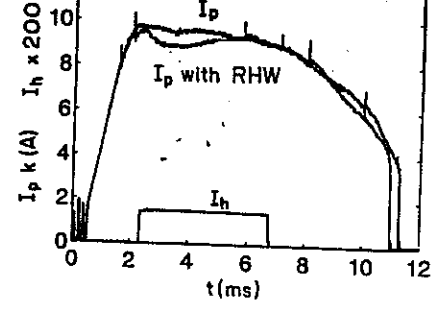


Fig. 2 - Time evolution of plasma current ( $I_p$ ) and RHW current ( $I_h$ ).

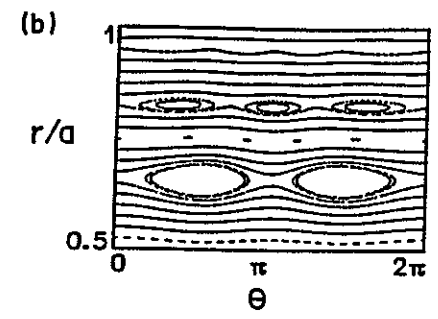
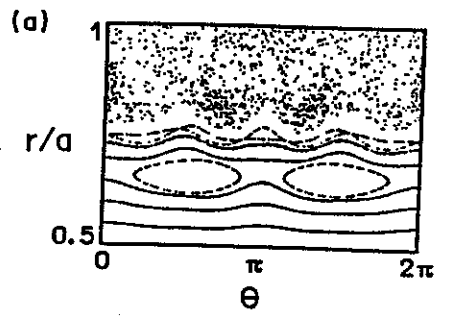


Fig. 3- Poincaré maps showing the poloidal magnetic field line configurations with RHW (a) and without RHW (b).

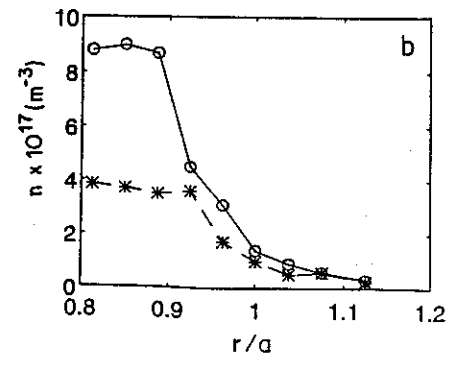
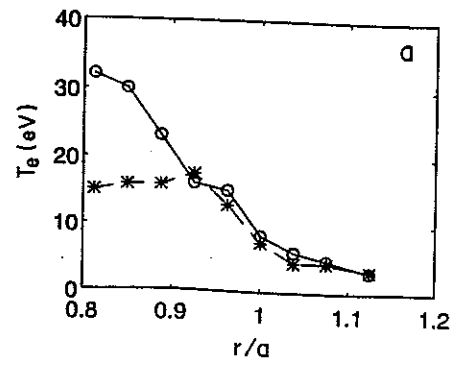


Fig. 4- Radial profiles of electron temperature with (\*) and without (o) RHW (a). The same for plasma density profiles (b).

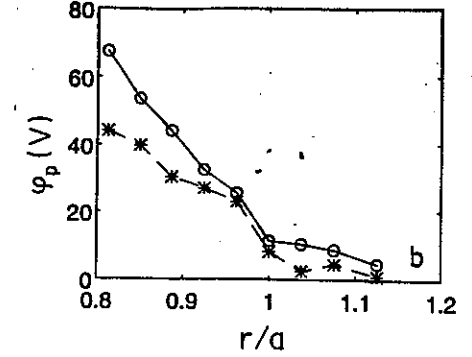
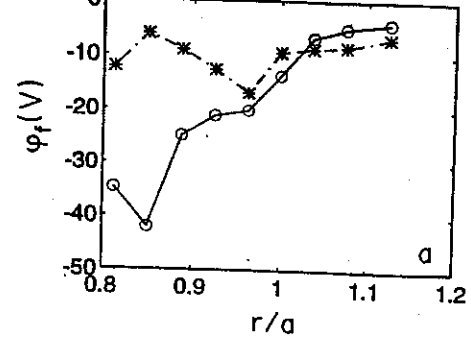


Fig. 5- Radial profiles of fluctuating potential with (\*) and without (o) RHW (a). Radial profiles for plasma potential with (\*) and without (o) RHW (b).

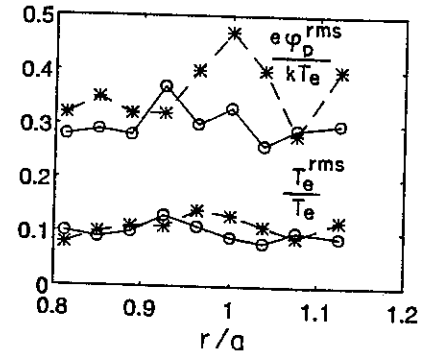


Fig. 6- Edge radial profiles of electron temperature fluctuation rms amplitudes normalized to local mean value of temperature, with (\*) and without (o) RHW. The same for plasma potential.

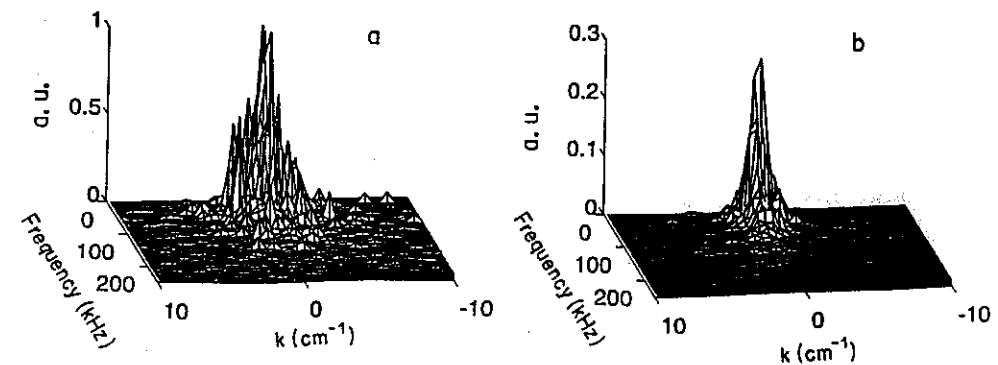


Fig. 7-  $S(k, f)$  spectra for density fluctuations at  $r/a = 0.89$  without RHW (a) and with RHW (b).



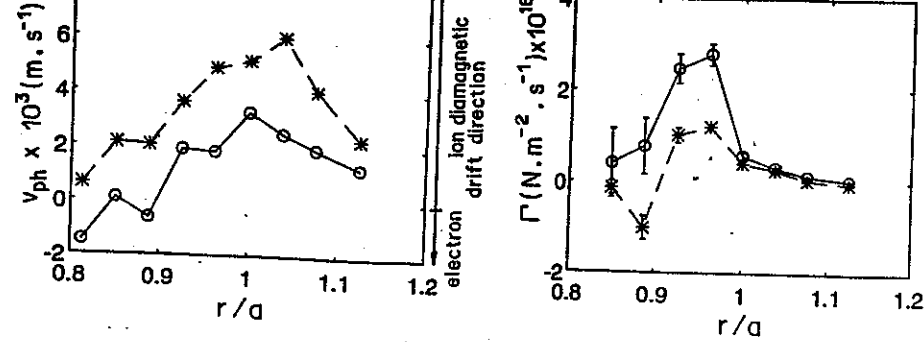


Fig.8- Phase velocity profiles for plasma potential fluctuations with (\*) and without (o) RHW.

Fig.9- Induced particle flux profiles with (\*) and without (o) RHW.

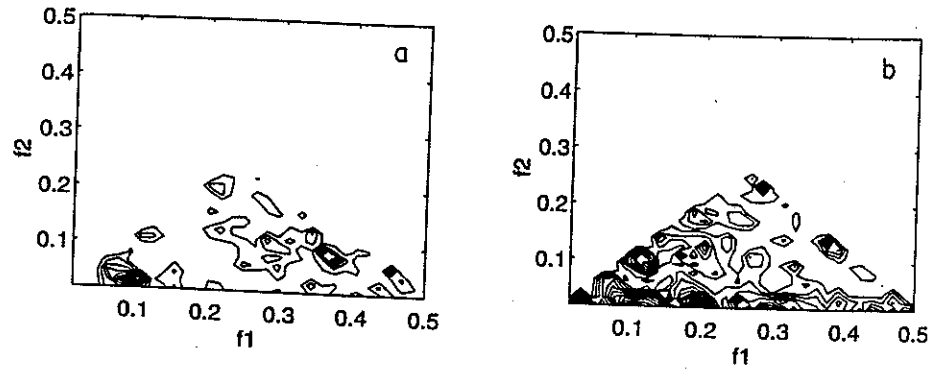


Fig. 10- Bicoherence for ion saturation current fluctuations at  $r/a = 0.92$  with (a) and without (b) RHW. Data filtered at 250 kHz and frequencies normalized to Nyquist frequency.

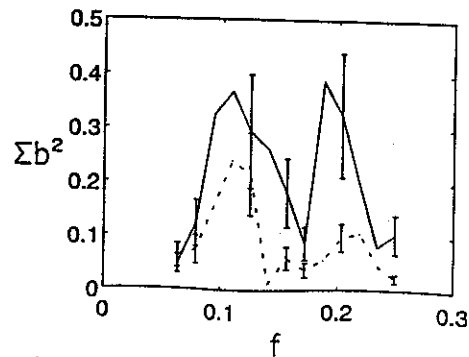


Fig. 11- Integrated bicoherence for ion saturation current fluctuations with (....) and without (—) RHW at  $r/a = 0.92$ . Data filtered at 250 kHz and frequencies

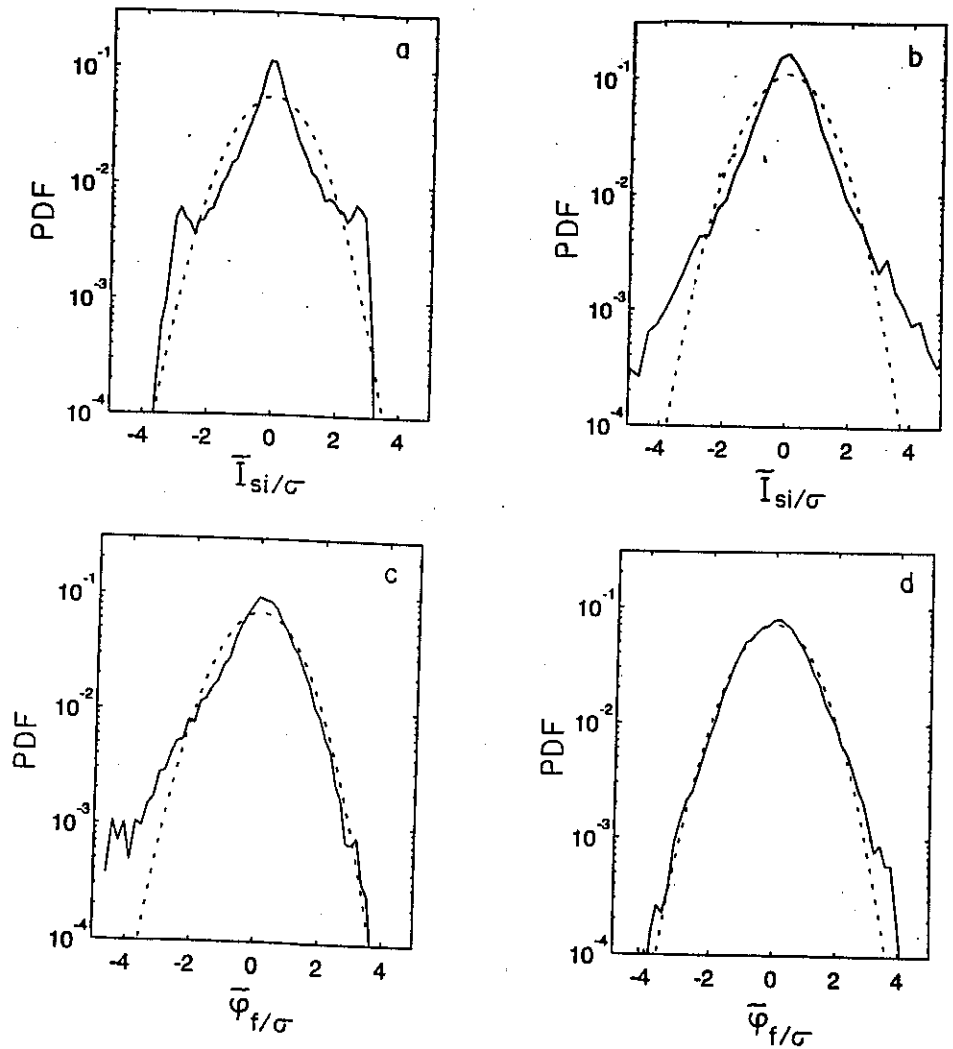


Fig.12- Probability distribution functions for ion saturation current, without (a) and with RHW (b), as a function of fluctuation amplitude normalized to the respective standard deviation. The same for floating potential fluctuations, (c) and (d). The dashed curves represent Gaussian with the same standard deviation.

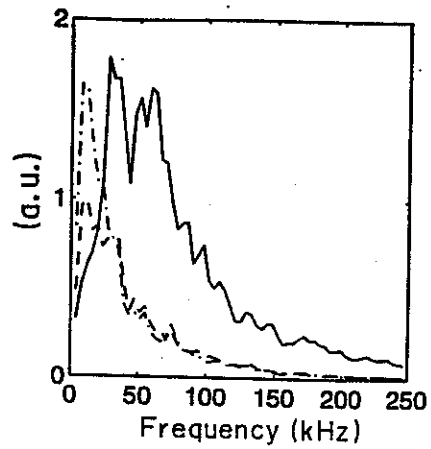


Fig.13- Spectra of density(—) and plasma potential (-.-.-) at  $r/a = 0.81$ , and poloidal magnetic fluctuations ( ) at  $r/a = 1.03$  with RHW utilization.

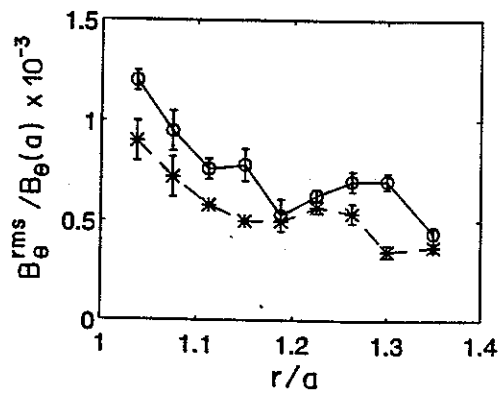


Fig.14- Radial profiles of the normalized magnetic poloidal fluctuations with (\*) and without (o) RHW.

Nuclear Fusion **35**, 59 (1995).

- <sup>29</sup> X. Z. Yang, B. Z. Zhang, A. J. Wootton, P. M. Schoch, B. Richards, D. Baldwin, D. L. Brower, G. G. Castle, R. D. Hazeltine, J. W. Heard, R. L. Hickok, W. L. Li, H. Lin, S. C. McCool, V. J. Simcic, Ch. P. Ritz, and C. W. Yu, Phys. Fluids **B3**, 3448 (1991).
- <sup>30</sup> T. L. Rhodes, C. P. Ritz, and R. D. Bengtson, Nucl. Fusion **33**, 1147 (1993).
- <sup>31</sup> A. S. Ware et al., Phys. Fluids **B4**, 877 (1992).
- <sup>32</sup> S. Raychoudhury and P. K. Kaw Phys. Fluids **B1**, 1646 (1989).
- <sup>33</sup> A. Nicolai, F. Schöngen, D. Reiter, Plasma Physics **27**, 1479 (1985).
- <sup>34</sup> Fielding, A.J. Wootton Physica Scripta **23**, 97 (1981).
- <sup>35</sup> Ph. van Milligen, C. Hidalgo, and E. Sanchez, Phys. Rev. Lett. **74**, 395 (1995).
- <sup>36</sup> Pulsator Team, Nuclear Fusion **25**, 1059 (1985).
- <sup>37</sup> C. Robinson, Nuclear Fusion **25**, 1101 (1985).
- <sup>38</sup> G. Vayakis N. Fusion, **33**, 547 (1993).
- <sup>39</sup> J. S. Sarff, S. A. Hokin, H. Ji, S.C. Prager, and C.R. Sovinec, Phys. Rev. Lett. **73**, 3670 (1994).
- <sup>40</sup> G. Li, J.R. Drake, H. Bergsaker, J.H. Brzozowski, G. Hellblom, S. Mazur. A. Möller, and P. Nordlund, Phys. Plasmas **2**, 2615 (1995).
- <sup>41</sup> H. Lin, Turbulence and Transport Studies in the Edge Plasma of the TEXT Tokamak Rep. FRCR N 401, University of Texas, Fusion Research Center, Austin, TX (1991).
- <sup>42</sup> N. Ohyabu et al., Phys. Rev. Lett. **58**, 120 (1987).

- <sup>43</sup> M. Malacarne et al, Fluctuations During JET Discharges with H-Mode, Rep. JET-P, JET Joint Undertaking, Abingdon, Oxfordshire (1987).
- <sup>44</sup> H. Tasso, Plasma Physics, **17**, 1131 (1975).
- <sup>45</sup> M.F.F. Nave et. al. Nuclear Fusion **32**, 825 (1992).
- <sup>46</sup> A. Tomimura, R. M. O. Galvão, Nuclear Fusion **33**, 1089 (1993).
- <sup>47</sup> M. V. A. P. Heller and I. L. Caldas, Il Nuovo Cimento **14D**, 695 (1992).
- <sup>48</sup> A. V. Filippas, R. D. Bengtson, G. X. Li, M. Meier, Ch. P. Ritz, E. J. Powers, Phys. Plasmas, **2**, 839 (1995).